Green Chemistry

ROYAL SOCIETY OF CHEMISTRY

COMMUNICATION

View Article Online
View Journal | View Issue

Cite this: *Green Chem.*, 2024, **26**, 8685

Received 31st May 2024,
Accepted 5th July 2024

DOI: 10.1039/d4gc02657h

rsc.li/greenchem

Expanding the toolbox of Baeyer–Villiger and flavin monooxygenase biocatalysts for the enantiodivergent green synthesis of sulfoxides†

Jingyue Wu, [a] Silvia Anselmi, [a] Alexandra T. P. Carvalho, [b] Jill Caswell,[b] Derek J. Quinn,[b] Thomas S. Moody*[b,c] and Daniele Castagnolo *[a]

Two new monooxygenase biocatalysts, the Baeyer–Villiger monooxygenase BVMO145 and the flavin monooxygenase FMO401 from Almac library, have been found to catalyse the enantiodivergent oxidation of sulfides bearing N-heterocyclic substituents into sulfoxides under mild and green conditions. The biocatalyst BVMO145 provides (*S*)-sulfoxides while the flavin monooxygenase FMO401 affords (*R*)-sulfoxides with good conversions and high ee.

Chiral sulfoxides are a ubiquitous class of compounds that find broad applications in pharmaceutical chemistry,[1] and they constitute the key structural motif of many pharmaceutics, including the drugs armodafinil,[2] flosequinan and esomeprazole (Fig. 1).[3] The absolute configuration of the sulfoxide moiety has a key impact on their chemical and biological properties. Optically pure sulfoxides also find use as catalysts, building blocks and chiral ligands in organic chemistry.[3–8] The main approach to synthesise enantiopure sulfoxides consists of the asymmetric oxidation of a prochiral sulfide precursor. Classic oxidation methods employ metal oxidants such Ti, V, Mn or Cu in the presence of appropriate chiral ligands (*i.e.* salen ligands and chiral Schiff bases).[1,9,10] More recently, the need to access such important compounds *via* milder and greener strategies has driven the interest of both academia and industry to exploit enzymes as biocatalysts in sulfoxidation reactions.[11]

Baeyer–Villiger monooxygenases (BVMOs) and flavin-containing monooxygenases (FMOs) are oxidative enzymes that belong to a broader class of enzymes called flavoprotein monooxygenases (FPMO). To date, there are eight subclasses of FPMOs (Groups A to H), which are differentiated by both structural and functional features.[12–15] Enzymes belonging to Groups A and B rely on the tightly bound flavin adenosine dinucleotide (FAD) prosthetic group and NAD(P)H as electron donors for their oxidative activity. The FPMOs in Groups A and B are single-component enzymes, capable of regenerating the active site without the need for external recycling systems, making them attractive potential biocatalysts. BVMOs and FMOs are classified as Group B FPMOs,[12–15] and even in cases of a low degree of sequence similarity, they share common structural features such as a Rossmann-like three-layer ββα sandwich domain for FAD binding, a NAD(P)H binding site, and a further ββα sandwich binding domain for the pyridine nucleotide.

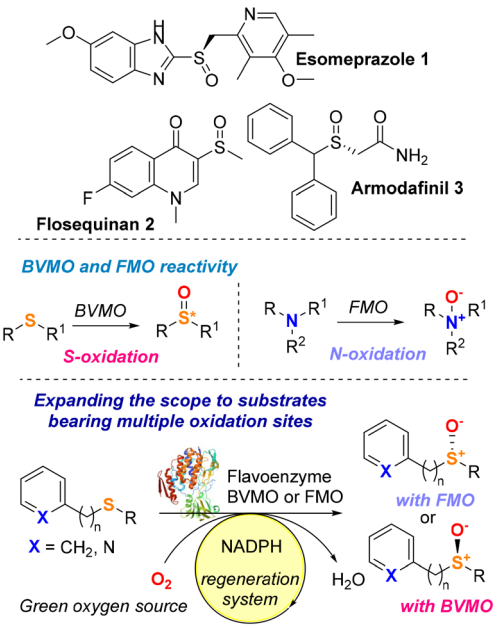

Fig. 1 Biocatalytic approaches for the synthesis of enantiomerically pure sulfoxides.

[a]*Department of Chemistry, University College London, 20 Gordon Street, WC1H 0AJ London, UK. E-mail: d.castagnolo@ucl.ac.uk*
[b]*Department of Biocatalysis & Isotope Chemistry, Almac, 20 Seagoe Industrial Estate, Craigavon, BT63 5QD, UK. E-mail: tom.moody@almacgroup.com*
[c]*Arran Chemical Company Limited, Unit 1 Monksland Industrial Estate, Athlone, Co. Roscommon, Ireland*

† Electronic supplementary information (ESI) available. See DOI: https://doi.org/10.1039/d4gc02657h

BVMO and FMO enzymes have attracted a lot of attention from the scientific community because they provide safer, chemo- and stereoselective, and overall, more sustainable alternatives compared to the traditional methods for Baeyer–Villiger transformations and heteroatom oxidations, especially *S*- and *N*-oxides.[12,14] BVMOs and FMOs have been used since the 1960s to catalyse a variety of oxidative transformations and several extensive reviews that summarise the use of these enzymes can be found in the literature.[16–20] Depending on the nature of the substrate and the protonation state of peroxyflavin FAD-OO(H), BVMOs and FMOs can catalyse the electrophilic addition of oxygen onto sulfur or nitrogen substrates, leading to sulfoxides or *N*-oxide derivatives. BVMO-catalysed sulfoxidations make up most of the work reported in the literature, as these enzymes have traditionally been under scrutiny for their biocatalytic properties far more than FMOs. On the other hand, *N*-oxidations are more common with FMOs, as their physiological role is to metabolise nitrogen-containing toxins in organisms.[12–21] Although the ability of BVMOs to perform enantioselective sulfoxidations has been proven throughout the decades, the full biocatalytic potential of FMOs for the synthesis of enantiopure sulfoxides remains largely unexplored. Additionally, most reports on the chiral production of sulfoxides focus on substrates that do not bear nitrogen functional groups that could potentially lead to the formation of *N*-oxide side products. Therefore, the lack of a detailed study on the chemoselectivity of BVMOs and FMOs when reacted with multifunctional substrates means that the applicability of these FPMOs remains still limited to structurally simple prochiral sulfides.

With the aim to expand the toolbox of biocatalysts and the substrate scope of green sulfoxidation reactions, herein we describe the identification of two new monooxygenase biocatalysts (BVMO and FMO) able to catalyse under mild conditions the enantiodivergent and selective oxidation of various sulfide substrates, including compounds bearing both a sulfur atom and an N-heteroaryl functional group. *In silico* studies have been also carried out to rationalise the enantioselectivity of these biotransformations (Fig. 1).

The Almac selectAZyme™ library, consisting of 50 BVMO and 60 FMO biocatalysts, either wild type or engineered freeze-dried cell free extracts (CFE), was initially screened on the pyridine-containing sulfide **4a**, bearing a sulfide moiety and a potentially oxidisable heteroaryl nitrogen. The sulfide **4a** (1.2 mM) was reacted with 10 g L^{-1} of the appropriate BVMO or FMO enzyme (cell free extract, CFE), 2.0 g L^{-1} glucose dehydrogenase (GDH), 5.5 eq. glucose and 2.0 mM $NADP^+$ in 50 mM Tris-HCl buffer at pH = 8.0. The screening results are reported in Fig. 2 and Table S1.† The conversion of the sulfide into the desired sulfoxide, the enantioselectivity and the formation of sulfone over-oxidised side products were determined by chiral HPLC. All BVMO and FMO enzymes oxidised the sulfide **4a** into the corresponding sulfoxide **5a**. Biocatalyst BVMO145 led to enantiomer **(*S*)-5a** with excellent >99% ee and 75% conversion and it showed remarkable chemoselectivity for sulfide oxidation since no traces of the sulfone **6** and the

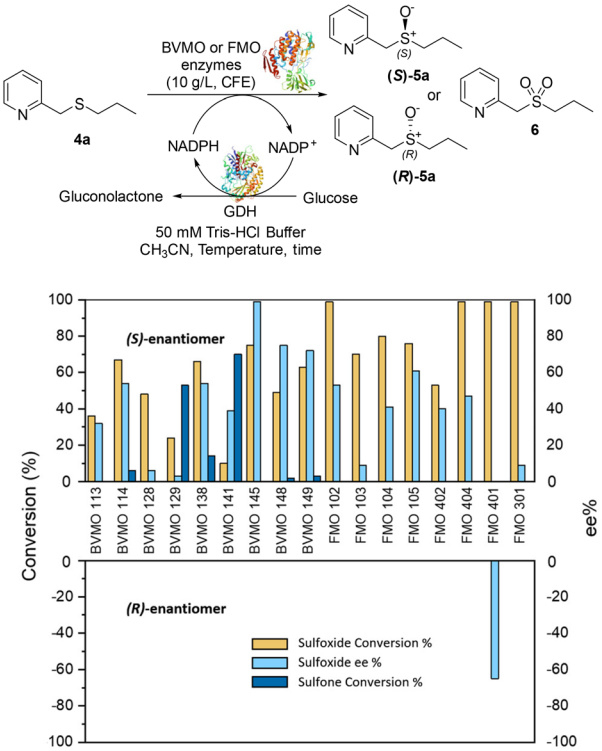

Fig. 2 Screening results of BVMOs and FMOs for asymmetric oxidation of **4a** to chiral sulfoxide **5a** and the corresponding sulfone **6**. Yellow bar: sulfoxide conversion % (determined by reversed phase HPLC using a Kromasil C18 column, monitored at 254 nm); sky-blue bar: ee % of **4a** (determined by chiral HPLC using a Chiralpak IC column, monitored at 254 nm); navy bar: sulfone side product conversion % (determined by reversed phase HPLC using a Kromasil C18 column, monitored at 254 nm). For information about the enzyme sequence, contact Prof. Thomas S. Moody at Almac by email (see ESI, page S2†).

N-oxide side products were observed.[22,23] In contrast, BVMO129 and BVMO141 showed negligible stereoselectivity in the oxidation of **4a** leading to the sulfone **6** as the major biotransformation product. Remarkably, biocatalyst FMO401 showed opposite enantioselectivity to BVMO145 providing the sulfoxide **(*R*)-5a** with excellent conversion (>99%) and good 65% ee. Interestingly, all FMO biocatalysts showed excellent activity on **4a** leading to sulfoxide **5a** with high conversion, but in most cases with low ee. No *N*-oxidation of the pyridine ring was observed for all the enzymes screened. Therefore, enzymes BVMO145 and FMO401 were selected for further substrate scope screening.

First, the optimization of the biotransformation conditions was conducted on substrate **4a** with biocatalyst BVMO145. The results are reported in Table 1.

The cofactor NADPH was generated *in situ* by adopting a glucose dehydrogenase (GDH)/glucose system. The concentration of $NADP^+$ was initially investigated and it was observed that lowering it to 0.06 mM (5 mol%) was sufficient for the reaction to take place without altering the product ee (>99%, Table 1, entry 3). The reduction of the GDH loading was then explored. When the GDH loading was reduced from 5.0 g L^{-1}

Table 1 Optimisation of BVMO145 catalysed sulfoxidation reaction conditions

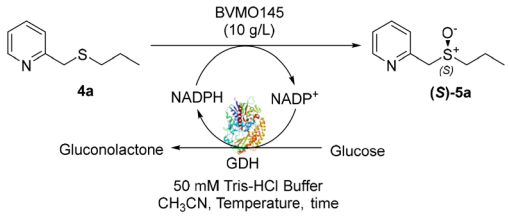

Entry	Substrate **4a** (mM)	$NADP^+$ (mM)	GDH (g L^{-1})	pH	*T* (°C)	Time (h)	Sulfoxide (*S*)-**5a** conv.[a] (%)	ee[b] (%)
1	1.2	0.18	2	8.0	30	18	90	>99
2	1.2	0.12	2	8.0	30	18	90	>99
3	1.2	0.06	2	8.0	30	18	90	>99
4	1.2	0.06	5	8.0	30	18	40	>99
5	1.2	0.06	1	8.0	30	18	93	>99
6	5.0	0.06	1	8.0	30	18	42	>99
7	10	0.06	1	8.0	30	18	12	>99
8	20	0.06	1	8.0	30	18	12	>99
9	40	0.06	1	8.0	30	18	10	>99
10	5.0	0.25	1	8.0	30	18	93	>99
11	10	0.50	1	8.0	30	18	70	>99
12	5.0	0.25	1	7.0	30	18	93	>99
13	5.0	0.25	1	9.0	30	18	>99	>99
14	**5.0**	**0.25**	**1**	**9.0**	**37**	**18**	**>99**	**>99**
15	**5.0**	**0.25**	**1**	**9.0**	**37**	**4**	**>99**	**>99**
16	5.0	0.25	1	9.0	37	1	71	>99
17[c]	5.0	0.25	1	8.0	30	18	<1	n.d.[d]
18[e]	5.0	0.25	1	8.0	30	18	<1	n.d.[d]
19	—	0.25	1	8.0	30	18	—	—

[a] Determined by reversed phase HPLC using a Kromasil C18 column, monitored at 254 nm. Based on the consumption of the sulfide. [b] Determined by chiral HPLC using a Chiralpak IC column, monitored at 254 nm. [c] Empty Pet28a vector *E. coli* CFE. Additional blank experiments on different sulfide substrates with empty Pet28a vector *E. coli* CFE are reported in the ESI (Table S2).† [d] n.d. = not determined. [e] Enzyme-free reaction.

(Table 1, entry 4) to 1.0 g L^{-1} (Table 1, entry 5), the conversion of **4a** to sulfoxide (***S***)**-5a** improved significantly from 40% to 93%. The optimal concentration of **4a** was also investigated to improve the efficiency of the method. Despite the excellent ee values, the increase of the concentration of **4a** to 5–40 mM led to (***S***)**-5a** with low conversions (Table 1, entries 6–9), while increasing the concentration of $NADP^+$ to 0.25–0.5 mM allowed the increase of the concentration of **4a** to 5–10 mM maintaining respectively excellent ee values (99%) and high conversions (Table 1, entries 10 and 11). Finally, the effects of pH and temperature on the biotransformation were investigated.

An increase of the pH from 8.0 to 9.0 led to a remarkable improvement of the conversion (>99%, Table 1, entries 12 and 13), while no differences were observed when the reaction was run at higher temperatures (Table 1, entry 14). However, carrying out the sulfoxidation at 37 °C allowed the reduction of the biotransformation time to 4 h (Table 1, entry 15) and the setting of the optimal reaction conditions. Finally, three control experiments were performed with empty pET28a vector *E. coli* CFE, enzyme-free and substrate **4a** free reactions to confirm the oxidizing activity of the enzymes (Table 1, entries 17–19). In all cases, no product (***S***)**-5a** was detected confirming the catalytic role of the enzyme in the biotransformation. A frequent issue reported in BVMO catalytic systems is that the low reactivity of the substrates can cause the spontaneous decomposition of peroxyflavin, with the release of hydrogen peroxide that can be responsible for side reactions, like *N*-oxidations. Remarkably, under the optimised conditions, no formation of side products (pyridine *N*-oxide) or decreased ee of (***S***)**-5a** was observed.[24]

With the optimal reaction conditions in hand, the scope of the BVMO145 and FMO401 enzymatic sulfoxidation was investigated (Table 2). Sulfides **4a–c** were converted in 18–24 h by BVMO145 into the corresponding (*S*)-sulfoxides (***S***)**-5a–c** with excellent ee values (>99%) and good to high conversions (Table 2, entries 1, 6 and 8). The biocatalyst FMO401 showed complementary enantioselectivity to BVMO145, affording enantiomers (***R***)**-5a** and **b** with high conversions and good to high ee values (Table 2, entries 2 and 7). Remarkably, FMO401 converted **4c** into (***R***)**-5c** with high ee (80%) and yield (93%), (Table 2, entry 9). The oxidation of substrates **4a** and **4c** with both biocatalysts proved to be selective towards the formation of the sulfoxide products **5a** and **5c**, while no formation of the sulfone side products **6a** and **6c**, arising from overoxidation of **5**, was observed. On the other hand, the enzymatic oxidation of the smaller sulfide **4b** led to the formation of **6b** in a variable amount when either BVMO145 or FMO401 was used (Table 2, entries 6 and 7).

The efficacy of BVMO145 was then compared with that of the biocatalysts TmCHMO and PAMO,[25,26] previously reported

Table 2 Substrate scope of flavoenzyme catalysed sulfoxidation

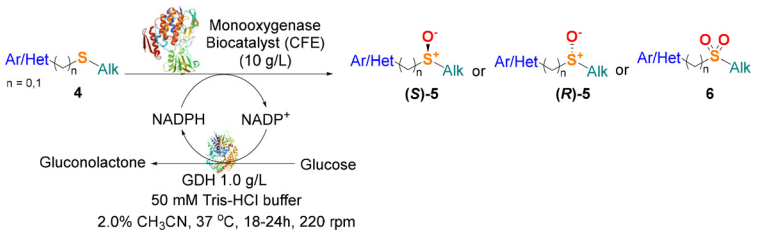

Entry	Sulfide **4** substrate	Biocatalyst	Sulfoxide **5** enantiomer	Sulfoxide **5** ee[a] (%)	Sulfoxide **5** yield[b] (%)	Sulfone **6** conv.[c] (%)
1	**4a** 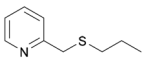	BVMO145	(***S***)-**5a**	>99	70 (99)[c]	0
2		FMO401	(***R***)-**5a**	64	72	0
3		BVMO145 W506A	(***R,S***)-**5a**	Racemic	3	0
4		TmCHMO	(***S***)-**5a**	>99	(40)[c]	60
5		PAMO	(***S***)-**5a**	84	53	32
6	**4b** 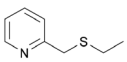	BVMO145	(***S***)-**5b**	>99	(65)[c]	35
7		FMO401	(***R***)-**5b**	60	30	26
8	**4c** 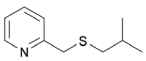	BVMO145	(***S***)-**5c**	>99	31	0
9		FMO401	(***R***)-**5c**	80	93	0
10	**4d** 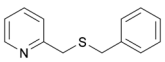	BVMO145	(***S***)-**5d**	n.d.[d]	<1	0
11		FMO401	(***R***)-**5d**	n.d.[d]	<1	0
12	**4e** 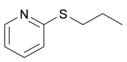	BVMO145	(***S***)-**5e**	n.d.[d]	6	0
13		FMO401	(***R***)-**5e**	46	67	0
14	**4f** 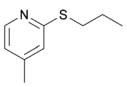	BVMO145	(***S***)-**5f**	n.d.[d]	<1	0
15		FMO401	(***R***)-**5f**	<1	57	0
16	**4g** 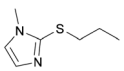	BVMO145	(***S***)-**5g**	76	57	0
17		FMO401	(***R***)-**5g**	<1	92	0
18	**4h**[e] 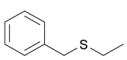	BVMO145	(***S***)-**5h**	>99	61	0
19		FMO401	(***R***)-**5h**	51	45	0
20		BVMO145 W506A	(***S***)-**5h**	n.d.[d]	<1	0
21		TmCHMO	n.d.[d]	n.d.[d]	<1	>99
22		PAMO	(***S***)-**5h**	>99	48	4
23	**4i** 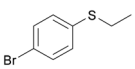	BVMO145	(***S***)-**5i**	>99	24	0
24		FMO401	(***S***)-**5i**	14	50	0
25	**4j**[e] 	BVMO145	(***S***)-**5j**	>99	24	0
26	**4k** 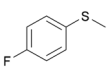	BVMO145	(***S***)-**5k**	>99	24	0
27		FMO401	(***S***)-**5k**	>99	22	0
28	**4l** 	BVMO145	(***S***)-**5l**	>99	76	0
29	**4m**[e] 	BVMO145	(***R***)-**5m**	>99	24	0
30		BVMO145 W506A	(***R***)-**5m**	n.d.[d]	<1	0
31		TmCHMO	n.d.[d]	n.d.[d]	<1	>99
32		PAMO	(***S***)-**5m**	22	52	4
33	**4n** 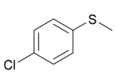	BVMO145	(***S***)-**5n**	n.d.[d]	<1	0

Table 2 *(Contd.)*

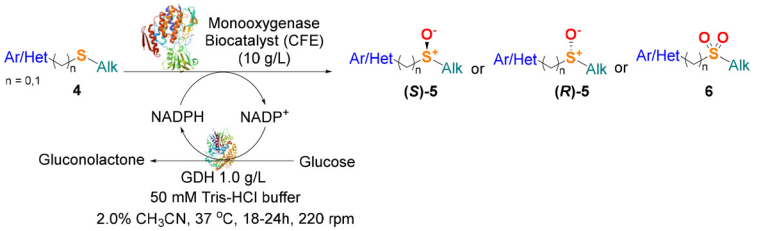

Entry	Sulfide **4** substrate	Biocatalyst	Sulfoxide **5** enantiomer	Sulfoxide **5** ee[a] (%)	Sulfoxide **5** yield[b] (%)	Sulfone **6** conv.[c] (%)
34	**4o** 	BVMO145	**(*S*)-5o**	n.d.[d]	<1	0

[a] Determined by chiral HPLC using a Chiralpak IG, IC or OD-H column, monitored at 254 nm. The absolute configuration was determined by comparing to the literature. [b] HPLC yield. Calculated using a reversed phase Agilent Eclipse Plus C18 column, monitored at 254 nm and methyl phenyl sulfoxide as an internal standard unless stated otherwise. [c] HPLC % conversion calculated from normal phase HPLC using a Chiralpak IG, IC or OD-H column. [d] n.d. = not determined. [e] Blank experiment with empty pET28a vector *E. coli* CFE is reported in the ESI (Table S2).†

in the literature for sulfoxidation reactions (Table 2, entries 4 and 5). Under the same reaction conditions, both TmCHMO and PAMO afforded the sulfoxide **(*S*)-5a** with high ee values and good conversions, even though slightly lower than those of BVMO145. However, a significant amount of the side product sulfone **6a** was obtained from these biotransformations (60% and 32% conversion respectively). The green metrics for the preparative biocatalytic sulfoxidation of the sulfides **4a** and **4c** are reported in Table 3.

The sulfide **4d** bearing a bulky benzyl group on the sulfur atom was not accepted by either BVMO145 or FMO401 (Table 2, entries 10 and 11), while the sulfides **4e** and **4f** bearing a pyridine directly on the sulfur atom proved to be poor substrates for both catalysts, with the exception of **4e** that

Table 3 Green metrics for the biocatalytic sulfoxidation of sulfides **4a** and **4c**

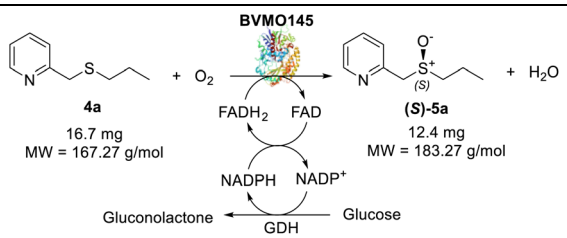

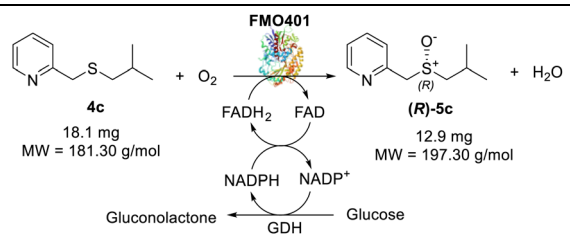

	MW (g mol^{-1})	Mass (mg)
Sulfide **4a**	167.27	16.7
Sulfoxide **5a**	183.27	12.4
O_2	32.00	—
CH_3CN	41.05	314
$NADP^+$	744.4	3.7
Glucose	180	180
Tris	121	118.5

Yield % = 68%[a]

$$\text{Atom economy}\,\% = \frac{183.27}{167.27 + 32} = 91.9\%$$

$$\text{Curzons RME}\,\% = \frac{12.4\ \text{mg}}{16.7\ \text{mg}} = 74.2\%$$

Kernel RME = 0.68 × 0.919 = 0.624

$$E\text{-Factor} = \frac{16.7 + 314 + 3.7 + 180 + 118.5 - 12.4}{12.4} = 50\ \text{kg kg}^{-1}$$

	MW (g mol^{-1})	Mass (mg)
Sulfide **4c**	181.3	18.1
Sulfoxide **5c**	197.3	12.9
O_2	32.00	—
CH_3CN	41.05	314
$NADP^+$	744.4	3.7
Glucose	180	180
Tris	121	118.5

Yield % = 65%[a]

$$\text{Atom economy}\,\% = \frac{197.30}{181.30 + 32} = 92.4\%$$

$$\text{Curzons RME}\,\% = \frac{12.9\ \text{mg}}{18.1\ \text{mg}} = 71.3\%$$

Kernel RME = 0.65 × 0.924 = 0.6

$$E\text{-Factor} = \frac{18.1 + 314 + 3.7 + 180 + 118.5 - 12.9}{12.9} = 48\ \text{kg kg}^{-1}$$

[a] Isolated yield after purification on silica gel (see the ESI† for preparative procedures).

was converted by FMO401 into **(*R*)-5e** with 46% ee (Table 2, entries 12–15). Such data clearly suggest that a methylene spacer between the pyridine ring and the sulfur atom is required by the enzyme to carry out the sulfoxidation reaction. On the other hand, the sulfide **4g** bearing an imidazole moiety was converted into **(*S*)-5g** in good yields and good ee by BVMO145, while in the presence of FMO401, **(*R*)-5g** was obtained with an excellent HPLC yield (92%), even if as a racemate (Table 2, entries 16 and 17). Again, no traces of sulfone **6** side products were observed in all the transformations catalysed by both BVMO145 and FMO401.

Molecular docking and molecular dynamics simulations were then carried out with selected substrates to interpret the substrate specificity and enantioselectivity displayed by the enzymes. A first computational analysis of the biocatalysts revealed that the substrate binding pockets of BVMO145 and FMO401 are considerably different. According to the accepted monooxygenase mechanism of action (Fig. 3a),[27,12] one of the electron lone pairs of the sulfur in substrates **4** attacks the peroxide group of C4a-hydroperoxyflavin and it is converted into the corresponding sulfoxide products **5**.

The BVMO145 active site is narrow with a well-documented H-bond between the catalytic arginine R340 and C4a-hydroperoxyflavin. Due to the steric hindrance of hydrophobic residues and NADP$^+$, BVMO145 allows substrate **4a** to only be oriented from the left side of C4a-hydroxyperoxyflavin, with the pro-(*S*) lone electron pair of the sulfur reacting with the oxygen of the hydroperoxide, leading to the formation of the enantiomer **(*S*)-5a** with excellent ee (>99%) (Fig. 3b). The W506 of BVMO145 seems to play a key role in the sulfoxidation of **4a**, since its replacement with an alanine (W506A mutation) led to the loss of catalytic activity and stereoselectivity (Table 2, entry 3). The W506 is located in the substrate tunnel and forms a hydrogen bond with the O2′ oxygen of the ribose moiety of the NADPH cofactor. Other residues within the substrate tunnel that interact with the pyridine moiety of the substrate **4a** are F500 and F299. In contrast to BVMO145, the FMO401 binding pocket is wider, and the propyl moiety of the substrate **4a** moves closer to the hydroperoxyl group, reacting *via* the pro-(*R*) lone electron pair of the sulfur and forming the **(*R*)-5a** sulfoxide product (Fig. 3c).

In FMO401, the substrate tunnel residue Y207 forms a H bond with the NADP$^+$/NADPH cofactor. Mutations of this tyrosine residue to valine or alanine (respectively the biocatalysts FMO402 and FMO404) have a great effect on the activity and selectivity of the enzyme, even if to a lesser extent than the mutation W507A in BVMO145. In fact, both mutants FMO402 and FMO404 provide the sulfoxide **(*S*)-5a** with good to high conversion compared to FMO401, but with lower enantioselectivity.

The computational analysis of the bulkier sulfide **4d** bearing a benzyl substituent on the sulfur atom revealed that **4d** is not able to fit the BVMO145 substrate binding tunnel near the isoalloxazine ring and thus to be oxidised into sulfoxide **5d** (Fig. S1†). On the other hand, the sulfide **4e** bearing a pyridine ring directly bonded to the sulfur atom is able to approach closely and bind the hydroperoxyl group in FMO401 affording **(*R*)-5e** with good 67% HPLC yield (Fig. 4b). However, in BVMO145, the pyridine ring of **4e** forms a charge-π interaction with the catalytic arginine residue leaving the sulfur atom too far from the C4a-hydroperoxyl group to allow a nucleophilic attack and, in turn, the formation of **(*S*)-5e** (Fig. 4a).

Intrigued by the opposite stereoselectivity of the BVMO145 and FMO401 biocatalysts, the enantioselective sulfoxidation of a series of aryl-alkyl sulfides **4h–o** was also investigated (Table 2). The biocatalyst BVMO145 retains activity and excellent enantioselectivity on most sulfide substrates affording the **(*S*)-5h–l** enantiomers with excellent enantiopurity (>99% ee) and good conversions (Table 2, entries 23, 25, 26 and 28).

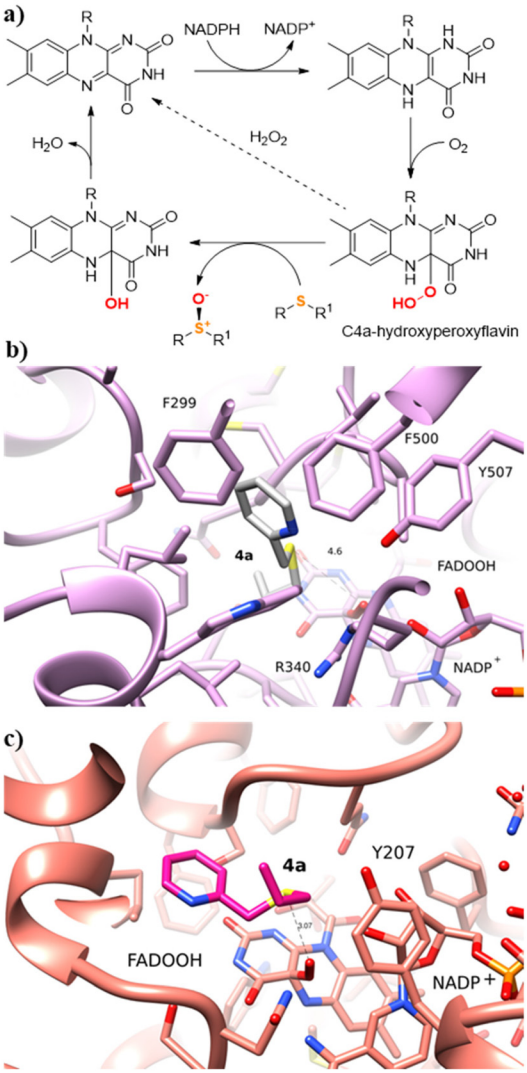

Fig. 3 (a) Mechanism of sulfoxidation by monooxygenase biocatalysts. (b) Sulfoxidation of **4a** by BVMO145. The active site of BVMO-145 only allows the binding of the substrate **4a** to the left side of C4a-hydroperoxyflavin. (c) Sulfoxidation of **4a** by FMO401. The hydroperoxyflavin is orientated to the sulfur lone electron pair pointing below giving the (*R*)-product. All hydrogens were omitted for clarity.

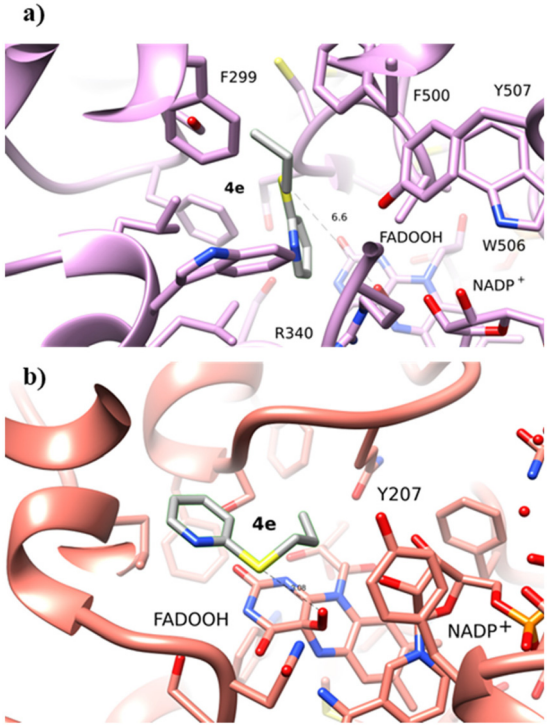

Fig. 4 (a) Sulfoxidation of **4e** by BVMO145. The orientation of **4e** is not correct to allow the sulfur nucleophilic attack on the hydroperoxyl group. (b) Sulfoxidation of **4e** by FMO401. The sulfide substrate **4e** is in the correct position to allow sulfoxide **5e** formation.

Interestingly, the oxidation of **4h** with PAMO showed opposite enantioselectivity to BVMO145, leading to the enantiomer (***R***)-**5h** with excellent enantioselectivity (>99%) and good conversion (Table 2, entry 22), while the oxidation of **4h** with TmCHMO afforded the side product sulfone **6h** as the only reaction product (Table 2, entry 21). The BVMO mutant W506A proved to be inactive also on **4h**, thus highlighting the key role of the W506 residue on the activity. Surprisingly, the sulfide **4m** bearing a *m*-methyl-substituent on the aromatic ring was oxidized by BVMO145 into the sulfoxide enantiomer (***R***)-**5m** (Table 2, entry 29). *In silico* studies showed that the methyl-phenyl ring of sulfide **4m** forms a charge-π interaction with the catalytic arginine residue R340 directing the approach of the substrate to the hydroperoxyl group to form the (***R***)-**5m** sulfoxide, albeit with a low yield as in the case of substrate **4e** (Fig. 5a and 4a).

Interestingly, PAMO showed again opposite enantioselectivity to BVMO145, affording (***S***)-**5m**, even if with a moderate yield and ee. The biocatalyst FMO401 showed complementary enantioselectivity on substrates **4h** and **4i** which were converted into the corresponding (***R***)-**5h** and **5i** sulfoxides with good yields but low enantioselectivity. While FMO401 showed excellent enantiopreference in the oxidation of pyridine-containing sulfides, lower selectivity was observed with smaller thio-phenyl substrates.

Interestingly, sulfide **4k** was oxidised by FMO401 into the corresponding sulfoxide (***S***)-**5k** showing an opposite selectivity

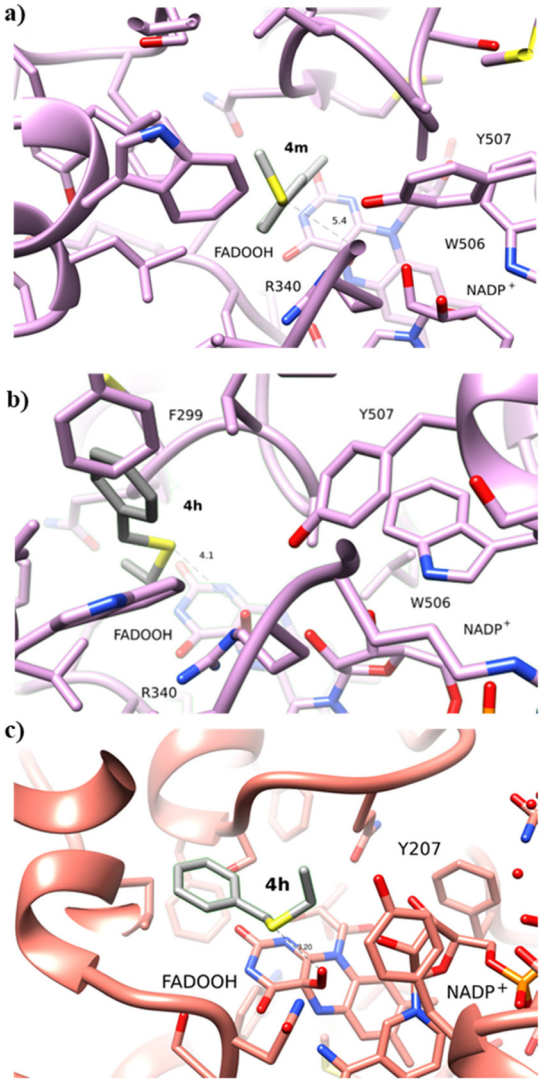

Fig. 5 (a) Binding of **4m** to BVMO145. The substrate **4m** forms a charge-π interaction with the catalytic R340; (b) binding of **4h** to BVMO145; (c) binding of **4h** to FMO401. The substrate **4h** binds with a similar position to substrate **4a**.

compared to other substrates (Table 2, entry 27). *In silico* studies clearly show the different enantiopreference of the biocatalysts BVMO145 and FMO401 on substrate **4h** through opposite interaction with C4a-hydroxyperoxyflavin (Fig. 5b and c).

Conclusions

Two new biocatalysts BVMO145 and FMO401 have been discovered in this work and they have been successfully used in the sulfoxidation of a variety of sulfide substrates. The two biocatalysts showed high enantio- and regio-selectivity in the oxidation of sulfide substrates bearing a pyridine ring, leading to the desired products in high ee (up to 99%) without the formation of sulfone or *N*-oxide side products. Remarkably, the two enzymes showed opposite enantiopreference, with the

enzyme BVMO145 affording the sulfoxide (*S*)-enantiomers and FMO401 catalysing the formation of the sulfoxide (*R*)-enantiomers. *In silico* studies allowed the rationalisation of the opposite enantioselectivity and substrate preference of the two biocatalysts. In conclusion, the identification of BVMO145 and FMO401 allows the expansion of the biocatalysis toolbox of oxidative monooxygenase biocatalysts to access enantiomerically pure sulfoxides under mild, selective and green conditions.

Author contributions

DC and TSM conceived and directed the project. JW and SA carried out the biocatalytic and synthetic experimental work. ATPC and DQ carried out and managed the computational studies. JC managed and carried out the biology work and prepared the biocatalysts.

Data availability

The data supporting this article have been included as part of the ESI.†

Conflicts of interest

There are no conflicts to declare.

Acknowledgements

We gratefully acknowledge BBSRC LIDo (BB/M009513/1) for PhD Studentships to SA. DC and JW acknowledge the China Scholarship Council programme (CSC, scholarship No 202008060037) for financial support to JW. Gecco Biotech and Prof. Marco Fraaije are gratefully acknowledged for providing the TmCHMO and PAMO biocatalysts.

References

1 J. Han, V. A. Soloshonok, K. D. Klika, J. Drabowicz and A. Wzorek, *Chem. Soc. Rev.*, 2018, **47**, 1307–1350.
2 C. J. Loland, M. Mereu, O. M. Okunola, J. Cao, T. E. Prisinzano, S. Mazier, T. Kopajtic, L. Shi, J. L. Katz, G. Tanda and A. H. Newman, *Biol. Psychiatry*, 2012, **72**, 405–413.
3 M. J. Kendall, *Aliment. Pharmacol. Ther.*, 2003, **17**, 1–4.
4 T. Jia, M. Wang and J. Liao, in *Sulfur Chemistry*, ed. X. Jiang, Springer International Publishing, Cham, 2019, pp. 399–427.
5 M. Mellah, A. Voituriez and E. Schulz, *Chem. Rev.*, 2007, **107**, 5133–5209.
6 I. Fernández and N. Khiar, *Chem. Rev.*, 2003, **103**, 3651–3706.
7 X. Salom-Roig and C. Bauder, *Synthesis*, 2020, **52**, 964–978.
8 B. M. Trost and M. Rao, *Angew. Chem., Int. Ed.*, 2015, **54**, 5026–5043.
9 P. Diter, S. Taudien, O. Samuel and H. B. Kagan, *J. Org. Chem.*, 1994, **59**, 370–373.
10 P. Pitchen, E. Dunach, M. N. Deshmukh and H. B. Kagan, *J. Am. Chem. Soc.*, 1984, **106**, 8188–8193.
11 (*a*) W. Mączka, K. Wińska and M. Grabarczyk, *Catalysts*, 2018, **8**, 624; (*b*) G. de Gonzalo, D. E. Torres Pazmiño, G. Ottolina, M. W. Fraaije and G. Carrea, *Tetrahedron: Asymmetry*, 2006, **17**, 130–135; (*c*) G. de Gonzalo, D. E. T. Pazmiño, G. Ottolina, M. W. Fraaije and G. Carrea, *Tetrahedron: Asymmetry*, 2005, **16**, 3077–3083; (*d*) A. Riebel, G. de Gonzalo and M. W. Fraaije, *J. Mol. Catal. B: Enzym.*, 2013, **88**, 20–25; (*e*) A. Riebel, G. de Gonzalo and M. W. Fraaije, *J. Mol. Catal. B: Enzym.*, 2013, **88**, 20–25; (*f*) S. Colonna, N. Gaggero, G. Carrea and P. Pasta, *Chem. Commun.*, 1997, 439–440; (*g*) I. Bassanini, E. E. Ferrandi, M. Vanoni, G. Ottolina, S. Riva, M. Crotti, E. Brenna and D. Monti, *Eur. J. Org. Chem.*, 2017, 7186–7189; (*h*) X. Wei, C. Zhang, X. Gao, Y. Gao, Y. Yang, K. Guo, X. Du, L. Pu and Q. Wang, *ChemistryOpen*, 2019, **8**, 1076–1083; (*i*) Y. Li, Y. Ma, P. Li, X. Zhang, D. Ribitsch, M. Alcalde, F. Hollmann and Y. Wang, *ChemPlusChem*, 2020, **85**, 254–257.
12 M. J. L. J. Fürst, A. Gran-Scheuch, F. S. Aalbers and M. W. Fraaije, *ACS Catal.*, 2019, **9**, 11207–11241.
13 N. M. Kamerbeek, D. B. Janssen, W. J. H. van Berkel and M. W. Fraaije, *Adv. Synth. Catal.*, 2003, **345**, 667–678.
14 C. E. Paul, D. Eggerichs, A. H. Westphal, D. Tischler and W. J. H. van Berkel, *Biotechnol. Adv.*, 2021, **51**, 107712.
15 C. E. Paul, D. Eggerichs, A. H. Westphal, D. Tischler and W. J. H. van Berkel, *Arch. Biochem. Biophys.*, 2014, **544**, 2–17.
16 R. M. Phelan, M. J. Abrahamson, J. T. C. Brown, R. K. Zhang and C. R. Zwick, *Org. Process Res. Dev.*, 2022, **26**, 1944–1959.
17 G. de Gonzalo and A. R. Alcántara, *Catalysts*, 2021, **11**, 605–629.
18 F. S. Aalbers and M. W. Fraaije, *ChemBioChem*, 2019, **20**, 20–28.
19 M. Bučko, P. Gemeiner, A. Schenkmayerová, T. Krajčovič, F. Rudroff and M. D. Mihovilovič, *Appl. Microbiol. Biotechnol.*, 2016, **100**, 6585–6599.
20 D. E. Torres Pazmiño, H. M. Dudek and M. W. Fraaije, *Curr. Opin. Chem. Biol.*, 2010, **14**, 138–144.
21 S. Thodberg and E. H. J. Neilson, *Catalysts*, 2020, **10**, 329–349.
22 The absolute configuration of the sulfoxides was determined by comparison with the optical rotatory values described in the literature and HPLC retention times.
23 S. Anselmi, A. T. P. Carvalho, A. Serrano-Sanchez, J. L. Ortega-Roldan, J. Caswell, I. Omar, G. Perez-Ortiz, S. M. Barry, T. S. Moody and D. Castagnolo, *ACS Catal.*, 2023, **13**, 4742–4751.
24 When the sulfide **4a** was reacted with *m*-CPBA (2 equiv.), the *N*-oxide side product was obtained in 15% yield (ESI, page S13†). This data clearly show the advantages of the biocatalytic *versus* chemical oxidation of sulfides into sulfoxides.

25 (*a*) G. de Gonzalo and A. Franconetti, *Enzyme Microb. Technol.*, 2018, **113**, 24–28; (*b*) E. Romero, J. R. Gómez Castellanos, A. Mattevi and M. W. Fraaije, *Angew. Chem., Int. Ed.*, 2016, **55**, 15852–15855; (*c*) Z.-G. Zhang, R. Lonsdale, J. Sanchis and M. T. Reetz, *J. Am. Chem. Soc.*, 2014, **136**, 17262–17272; (*d*) H. M. Dudek, G. de Gonzalo, D. E. Torres Pazmiño, P. Stepniak, L. S. Wyrwicz, L. Rychlewski and M. W. Fraaije, *Appl. Environ. Microbiol.*, 2011, **77**, 5730–5738.

26 TmCHMO shows 40% sequence similarity with BVMO145; PAMO shows 43% sequence similarity with BVMO145.

27 (*a*) R. D. Ceccoli, D. A. Bianchi and D. V. Rial, *Front. Microbiol.*, 2014, **5**, 25; (*b*) H. Leisch, K. Morley and P. C. K. Lau, *Chem. Rev.*, 2011, **111**, 4165–4222; (*c*) D. Sheng, D. P. Ballou and V. Massey, *Biochemistry*, 2001, **40**, 11156–11167; (*d*) I. Polyak, M. T. Reetz and W. Thiel, *J. Am. Chem. Soc.*, 2012, **134**, 2732–2741.